Photoionization of atoms encapsulated in endohedral ions $A@C_{60}^{\pm z}$

V. K. Dolmatov[1,*] and S. T. Manson[2,†]
[1]*Department of Physics and Earth Science, University of North Alabama, Florence, Alabama 35632, USA*
[2]*Department of Physics and Astronomy, Georgia State University, Atlanta, Georgia 30303, USA*
(Received 12 October 2005; published 3 January 2006)

Results of a theoretical study of photoionization cross sections and photoelectron angular asymmetry parameters of atoms confined by positively C_{60}^{+z} or negatively C_{60}^{-z} charged fullerene shells are presented. For negatively charged C_{60}, entirely new confinement resonances, termed *Coulomb confinement resonances*, that dominate the spectra of the encapsulated atoms are predicted. In addition, the effect of a negative C_{60} shell is to move some of the oscillator strength of the encapsulated atom from the discrete excitation region into the continuum. For positively charged C_{60}, the situation is much different; no Coulomb confinement resonances occur in the photoionization spectrum of the encapsulated atom, and charging the shell positively does nothing to the photoionization cross section (as a function of photon energy) except to increase the threshold energy. The findings result from model Hartree-Fock calculations of 1*s* photoionization of Ne confined by neutral, negative, and positive C_{60}.

DOI: 10.1103/PhysRevA.73.013201 PACS number(s): 36.40.Vz, 32.80.Dz, 32.80.Fb

I. INTRODUCTION

Endohedral fullerenes $A@C_{60}$—the nanostructure formations wherein a multielectron atom A is trapped inside a hollow fullerene cage C_{60}—are a subject of significant interest in recent years [1,2], because they exhibit properties that can lead to important applications in nanostructure science and technology. For example, it has been shown that C_{60} confinement could have some unique advantages in isolating the atom from its environment, thereby providing a building block for the qubits of the quantum computer [3]. A number of theoretical studies have explored the response of atoms A encapsulated in C_{60} cages to ionizing electromagnetic radiation, and phenomenology has been uncovered such as resonances in photoionization cross sections and photoelectron angular distributions of encapsulated atoms [4–10] termed *confinement resonances* [7] (see also a recent review paper [11] on this subject).

So far, however, the spectroscopy of confined atoms has been, perhaps, experimentally rather difficult to perform, and theoretical predictions have far outstripped experiment. It is likely that this situation will change, and that laboratory investigations of the spectroscopy of confined atoms will become available to test the theoretical predictions. In the meantime, we turn our attention to filling in aspects of the problem that so far have been ignored, such as the photoionization spectrum of the atom encapsulated inside a *charged* $C_{60}^{\pm z}$ shell: the endohedral ion $A@C_{60}^{\pm z}$. At this point in time, nothing is really known about these spectra, but their properties will clearly be of importance to understand given that investigations of endohedral ions, e.g., $N@C_{60}^{-z}$ [12–14] (and references therein) have been under way for some time now. When spectroscopy of such confined atoms becomes experimentally developed, it will be a matter of significant importance to the understanding to be capable of distinguishing which part of the photoionization spectrum of charged $A@C_{60}^{\pm z}$ is due to its confining $C_{60}^{\pm z}$ shell, and which to photoionization of the trapped atom A alone.

It is precisely the aim of this paper to explore theoretically features of the photoionization spectra of atoms encapsulated inside both endohedral positive ions (cations) and negative ions (anions), $A@C_{60}^{\pm z}$. We focus on uncovering effects that can occur in the photoionization process rather than to make the most precise calculations possible. To accomplish this end, we choose a system that is easier for us to study—$Ne@C_{60}^{\pm z}$—and we investigate 1*s* photoionization of the confined Ne. The choice is dictated by a number of reasons. To begin with, neutral endohedral fullerenes with encapsulated noble gas atoms do exist [15], and there is no reason that noble gas endohedral cations and anions should not exist as well. Secondly, the deepest 1*s* shell is clearly the least affected by the confining shell, and we use it to the advantage of our qualitative theory. Moreover, the choice of the deepest atomic shell with the ionization threshold of hundreds or more electron volts makes it possible to ignore completely the effect of dynamical screening in the photoionization of a confined atom by a fullerene shell [10]; the effect is very strong at photon energies around 24 eV, but rapidly falls off to negligible at much higher energies.

In our study, we perform calculations using Hartree-Fock (HF) wave functions to include charged confinement effects as a first step in understanding which aspects of the photoionization spectra are most interesting to study in greater depth. One important finding of the research is the observation of strong confinement resonances, termed *Coulomb confinement resonances*, which *dominate* the photoionization and photoelectron angular distribution spectra of encapsulated atoms inside a negatively charged C_{60}^{-z} cage. Another unexpected finding observes the redistribution of oscillator strengths of encapsulated atoms between the discrete and continuum spectrum depending on the magnitude and sign of the charge on a fullerene shell.

*Electronic address: vkdolmatov@una.edu
†Electronic address: smanson@gsu.edu

The atomic system of units ($e=\hbar=m_e=1$) is used throughout the paper.

II. THEORY

Our model approach to treat charged endohedral fullerenes $A@C_{60}^{\pm z}$ follows closely the approach previously used in various studies of neutral endohedral fullerenes (see, e.g., Refs. [5,11,16–18]).

First, for neutral C_{60}, the atom A is placed at the geometrical center of the shell. This is reasonable, since experimental studies of endohedral atoms $A@C_{60}$ show that noble gas atoms [15] and group-V atoms [19] are, as a rule, located at the center of the fullerene cage without any charge transfer to the cage. It is the very small van der Waals forces that cause the atom to be located at the center of the cage. These van der Waals forces are quite weak, compared to atomic (Coulomb) forces, so that they do not alter the ground state wave function of the encapsulated atom A appreciably. Since we consider the endohedral fullerene $Ne@C_{60}$ in this paper, we can reliably take the position of the Ne atom to be at the center of C_{60}. The C_{60} cage itself is modeled by a spherical, short-range, attractive shell-potential, $V^{cage}(r)$, of inner radius r_c, depth U_0, and thickness Δ:

$$V(r)=\begin{cases}-U_0<0, & \text{if } r\leqslant r_c+\Delta,\\ 0, & \text{otherwise.}\end{cases} \tag{1}$$

In accordance with Ref. [20], the radius $r_c\approx 3.04$ Å ≈ 5.8 a.u. and the thickness $\Delta\approx 1$ Å ≈ 1.9 a.u., whereas $U_0=8.22$ eV [5]; this choice reproduces the experimental electron affinity of 2.65 eV for C_{60} [21].

Second, to account for effects of a charged shell $C_{60}^{\pm z}$, we assume that the extra charge z is evenly distributed over the entire outer surface of C_{60}. Correspondingly, the entire model potential $V^{eff}(r)$ in the case of charged $C_{60}^{\pm z}$ is

$$V^{eff}(r)=V^{cage}(r)+V^{z}(r), \tag{2}$$

where $V^z(r)$ is the potential due to the charge on C_{60},

$$V^{z}(r)=\begin{cases}\dfrac{z}{r_c+\Delta}, & \text{if } 0\leqslant r\leqslant r_c+\Delta,\\ \dfrac{z}{r}, & \text{otherwise.}\end{cases} \tag{3}$$

Third, as in Ref. [5], to find electronic wave functions $\psi_{nlm}(\boldsymbol{r})=r^{-1}P_{nl}(r)Y_{lm}(\theta,\phi)$ and electronic energies ϵ_{nl} of the encapsulated atoms (where $n=\epsilon$ for continuum states), we incorporate the potential $V^{eff}(r)$ into the ordinary HF equations for a free atom (see, e.g., Ref. [22]). Correspondingly,

$$\left[-\frac{\Delta}{2}-\frac{Z}{r}+V^{eff}(r)\right]\psi_i(\boldsymbol{r})+\sum_{j=1}^{N}\int\frac{\psi_j^*(\boldsymbol{r}')}{|\boldsymbol{r}-\boldsymbol{r}'|}\times[\psi_j(\boldsymbol{r}')\psi_i(\boldsymbol{r})-\psi_i(\boldsymbol{r}')\psi_j(\boldsymbol{r})]d\boldsymbol{r}'=\epsilon_i\psi_i(\boldsymbol{r}). \tag{4}$$

Fourth, to calculate photoionization spectra of the confined atoms due to the radiation of frequency ω, the HF wave functions and energies, solutions of Eq. (4), are plugged into the ordinary formulae for photoionization cross sections $\sigma_{nl}(\omega)$ and photoelectron angular $d\sigma_{nl}/(\omega)d\Omega$ distributions for free atoms (see, e.g., Ref. [22]).

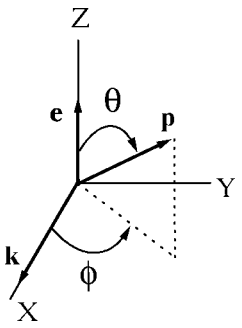

FIG. 1. Angles θ and ϕ in Eqs. (6) and (8) as relative to the photoelectron momentum **p**, photon momentum **k**, and photon polarization vector **e**.

Finally, since we focus on photon energies that are ~ 1 keV, we use the dipole approximation for the calculation of the total photoionization cross section of a nl subshell of the atom. For photoelectron angular distributions, we go beyond the dipole approximation by accounting for electric dipole-quadrupole interference effects as well, since a recent striking discovery has shown that these (usually ignored), nondipole effects are often big even at as low photon energies as hundreds or even tens of eV [23]. Correspondingly, for the total $\sigma_{nl}(\omega)$ and differential $d\sigma_{nl}/d\Omega$ photoionization cross sections of a nl subshell of the atom, we write [24]

$$\sigma_{nl}(\omega)=\frac{4\pi^2\alpha N_{nl}}{3(2l+1)}\omega[lD_{l-1}^2+(l+1)D_{l+1}^2], \tag{5}$$

$$\frac{d\sigma_{nl}}{d\Omega}=\frac{\sigma_{nl}}{4\pi}\left[1+\frac{\beta_{nl}}{2}(3\cos^2\theta-1)\right]+\Delta E_{12}, \tag{6}$$

where the latter equation assumes 100% linearly polarized light. In these equations, α is the fine structure constant, N_{nl} is the number of electrons in a nl subshell, $D_{l\pm1}$ is a radial dipole photoionization amplitude,

$$D_{l\pm1}=\int_0^\infty P_{\epsilon l\pm1}(r)rP_{nl}(r)dr, \tag{7}$$

β_{nl} is the dipole photoelectron angular asymmetry parameter, and ΔE_{12} is the nondipole (i.e., electric dipole-quadrupole) interference term,

$$\Delta E_{12}=\frac{\sigma_{nl}}{4\pi}(\delta_{nl}+\gamma_{nl}\cos^2\theta)\sin\theta\cos\phi. \tag{8}$$

In the latter equation, the spherical angles θ and ϕ are defined in relation to the direction of the photon momentum **k**, photoelectron momentum **p**, and photon polarization vector **e**, as in Fig. 1. From Ref. [24], for nonrelativistic ns photoionization, $\beta_{ns}=2$, $\delta_{ns}=0$, whereas

$$\gamma_{ns}=3k\frac{Q_{ns\to d}}{D_{ns\to p}}\cos(\eta_d-\eta_p). \tag{9}$$

Here, η_d and η_p are phase shifts of partial ϵd and ϵp photoelectron wave functions, correspondingly, whereas $D_{ns\to\epsilon p}$ is

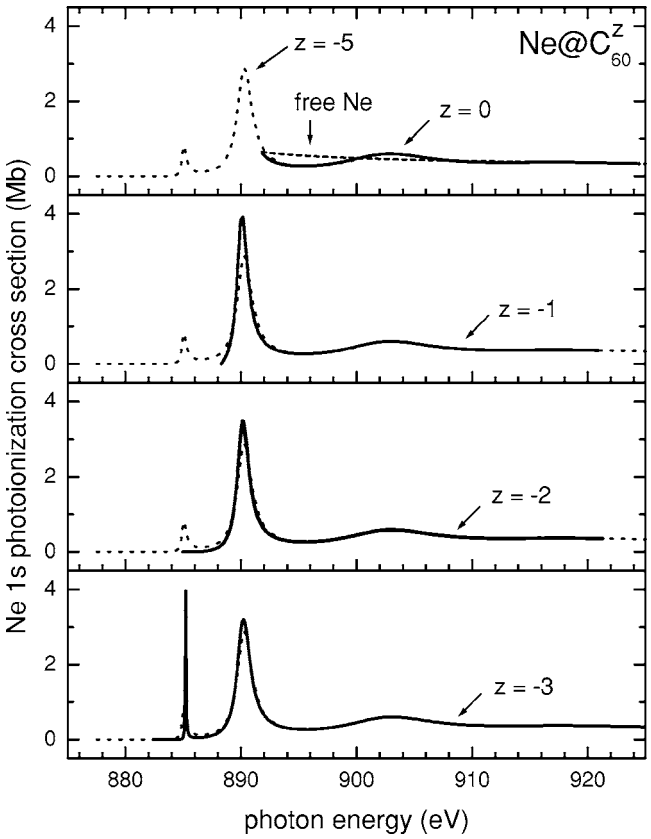

FIG. 2. Calculated HF results for the 1*s* photoionization of free Ne, as well as that of Ne from neutral Ne@C_{60} (z=0) and from the Ne@C_{60}^{z} anion with z=−1, −2, −3, and −5 (dotted line), as indicated.

the radial dipole photoionization amplitude [Eq. (7)] and $Q_{n\to\epsilon d}$ is the radial quadrupole photoionization amplitude:

$$Q_{ns\to\epsilon d} = \int_0^\infty P_{\epsilon d}(r) r^2 P_{nl}(r) dr. \tag{10}$$

III. RESULTS AND DISCUSSION

A. Endohedral anions: Coulomb confinement resonances

1. Photoionization cross section: σ_{1s} of Ne

Calculated results for a Ne 1*s* photoionization cross section, $\sigma_{1s}(\omega)$, from the Ne@C_{60}^{z} anion (z=−1, −2, −3, and −5) are shown in Fig. 2 along with calculated data for neutral Ne@C_{60} (z=0) and free Ne. For free Ne, we get a monotonically decreasing $\sigma_{1s}(\omega)$ with a threshold value of about 0.56 Mb. For neutral Ne@C_{60}, we get confinement resonances in $\sigma_{1s}(\omega)$ of Ne. Such resonances were predicted and investigated thoroughly earlier (Ref. [11] and references therein). Confinement resonances are due to the interference of the photoelectron waves going directly out, and scattered off the inner and outer walls of the C_{60} confining shell. The interference due to these three outgoing waves yields a cross section of the encapsulated atom with maxima and minima centered roughly about the photoionization cross section of a free atom.

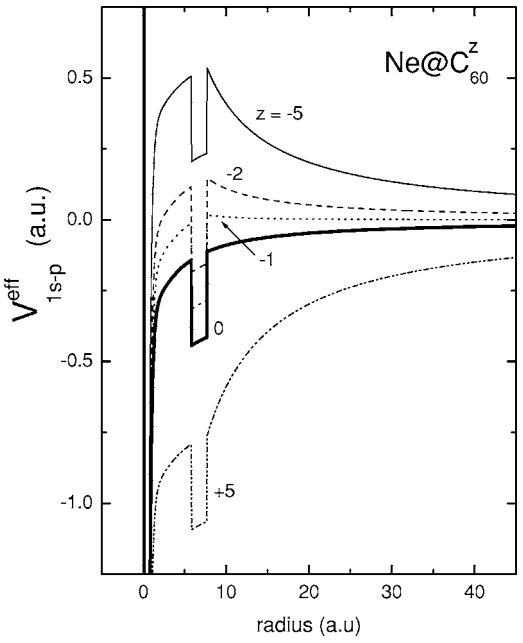

FIG. 3. Direct (Hartree) part of the effective potential $V^{eff}(r)$ [Eq. (2)] "seen" by a ϵp electronic wave arising from Ne 1*s* photoionization of Ne@C_{60}^{z} for z=−5, −2, −1, 0, and +5.

For an endohedral anion, Ne@C_{60}^{z} ($z<0$), the situation is affected dramatically by increasing the negative charge z on C_{60}^{z}. First, as the negative charge on C_{60} is increased just to z=−1, there appears a new, strong resonance structure in a lower-energy wing of $\sigma_{1s}(\omega)$, at $\hbar\omega\approx 890$ eV. As z keeps growing, the resonance structure is slowly broadening while slightly decreasing in height and, starting from z=−3, a new, sharp resonance comes up in $\sigma_{1s}(\omega)$ at yet lower energy, $\hbar\omega\approx 885$ eV. Likewise, the formerly discussed strong resonance structure, the new resonance becomes lower and broader with increasing negative z (compare results for z=−3 and z=−5).

Second, and this is quite striking, each subsequent increase in negative z is seen to add a new, lower-energy part to the former curve of $\sigma_{1s}(\omega)$ versus photon energy, while leaving the higher-energy part of the graph almost intact. The implication is that the effect of placing a negative charge onto the C_{60} surface is to move some of the oscillator strength of the encapsulated atom from the discrete excitation region into the continuum. In a sense, a negatively charged shell C_{60}^{z} ($z<0$) acts, as it were, a "magnifying glass (the shell itself) with adjustable index of refraction (the negative charge on the anion)," because it allows one to "see" the part of the oscillator strength of a confined atom that otherwise is hidden for the observer. Note that this effect is similar but opposite to the effect found some time ago [25] in the photoionization of inner shells of free *positive* ions. In the latter case, the effect of the increasing positive charge of the ion by removal of outer electrons, as compared to neutral atoms, was to move some of the oscillator strength of the atom from the continuum into the discrete excitation region.

To understand these striking features in the behavior of $\sigma_{1s}(\omega)$ with increasing negative z, it is helpful to explore the evolution in the potential $V^{eff}(r)$, Eq. (2), "seen" by an

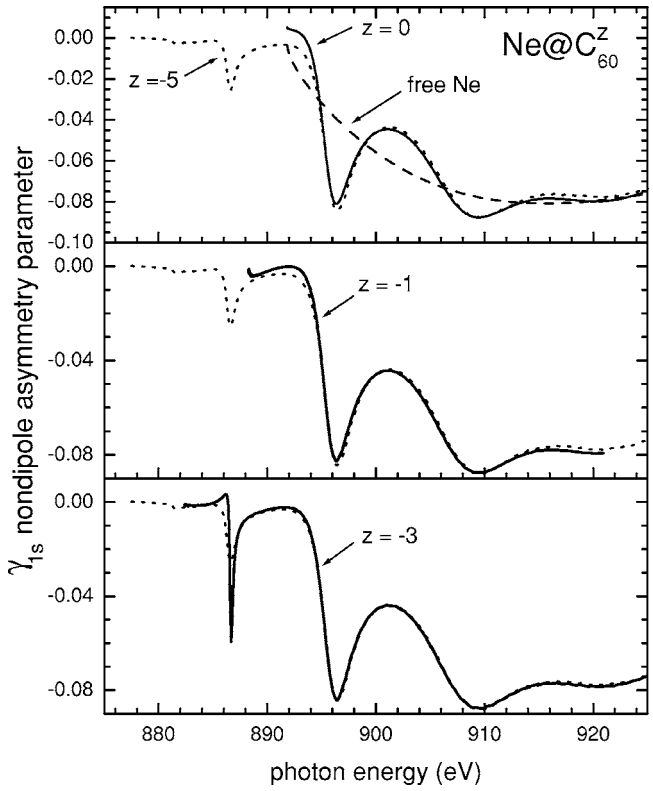

FIG. 4. Nondipole photoelectron angular asymmetry parameter $\gamma_{1s}(\omega)$ for 1s photoionization of free Ne, Ne from neutral Ne@C_{60} as well as Ne from the endohedral anion Ne@C_{60}^{z} ($z<0$), as indicated.

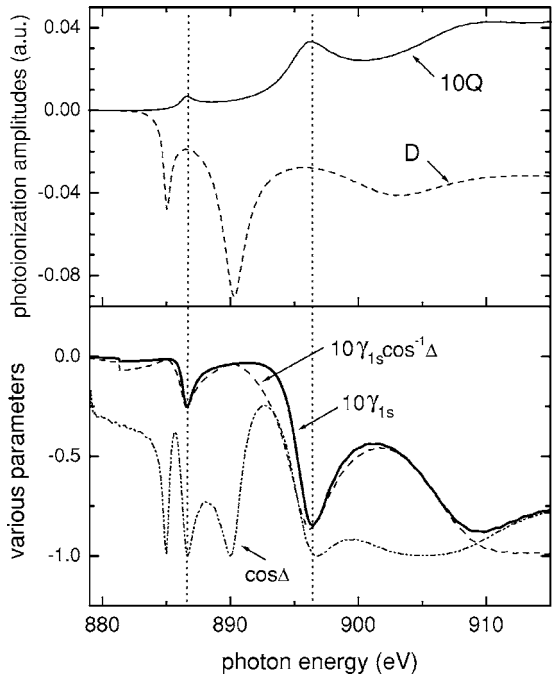

FIG. 5. Ne 1s nondipole photoelectron angular asymmetry parameter $\gamma_{1s}(\omega)$ along with its various components from Eq. (9)—the dipole D and quadrupole Q amplitudes and $\cos\Delta$ ($\Delta=\delta_2-\delta_1$)—arising from Ne photoionization in the Ne@C_{60}^{-5} anion.

ejected Ne 1s photoelectron for various values of z. The direct (Hartree) part of V^{eff} is shown in Fig. 3 for various z. For endohedral anions, V^{eff} is characterized not only by a common potential well between $r=5.8$ and $r=7.7$ a.u. for all z (this models the C_{60} shell itself), but also by the potential *barrier* (split by the well) in the positive plane of $V^{eff}(r)$. The latter is owing to the extra potential $V^{z}(r)$ [Eq. (3)], which is due to the negative charge z on the outer surface of C_{60}. This engenders reflection of the continuum photoelectron wave from the split Coulomb barrier causing additional kinds of confinement resonances (resonances at $\hbar\omega\approx 890$ and 885 eV in Fig. 2). We term these resonances "Coulomb confinement resonances" since they owe their existence to the confinement brought about by the Coulomb potential barrier of the charged shell. Coulomb confinement resonances dominate the ordinary confinement resonances (compare, e.g., the latter at $\hbar\omega\approx 903$ eV with the Coulomb confinement resonance around 890 eV). It is clear that the position and shape of Coulomb confinement resonances intimately involves the C_{60} shell as well. Thus, Coulomb confinement resonances are the result of the interference between the direct photoelectron wave, the reflected wave from the Coulomb *barrier*, and the reflected wave from the C_{60} shell (well).

As is readily deduced from Figs. 2 and 3, sharp Coulomb confinement resonances occur when the photoelectron energy is less than the barrier height. In addition, results for $z=-3$ and $z=-5$ indicate that in the energy region where the continuum wave has to penetrate the wider part of the Coulomb barrier, Coulomb confinement resonances are narrow, whereas they are much broader at higher energy, when the wave penetrates the narrow, near the top part of the barrier. Further, when the energy is above the barrier height, we get both types of resonances in the continuum: the large Coulomb confinement resonances at lower energies and the ordinary confinement resonance at higher energies. Clearly, this is a general phenomenon and will be in evidence in the photoionization of any atom, molecule, or ion, encapsulated by a negatively charged confinement.

Note further that the cross sections for Ne 1s photoionization from the endohedral anion are vanishingly small for energies below the potential barrier height (Fig. 3), as seen in Fig. 2, except for the Coulomb confinement resonances. This phenomenology is due to the Coulomb barrier, which does not allow the continuum wave functions to penetrate into the inner region where the 1s wave function has appreciable amplitude, thereby causing the overlap and the dipole matrix elements to be negligible. This too should be a general feature of photoabsorption by an object encapsulated by a negatively charged confinement.

2. Photoelectron angular asymmetry parameters: γ_{1s} of Ne

Results of the calculation of the 1s nondipole photoelectron angular asymmetry parameter $\gamma_{1s}(\omega)$ [Eq. (9)] for Ne from the endohedral Ne@C_{60}^{z} anion ($z<0$) along with data for neutral Ne@C_{60} are presented in Fig. 4. Like the situation with the photoionization cross section, the neutral shell C_{60} exhibits the ordinary confinement resonances in $\gamma_{1s}(\omega)$ that are centered roughly about the free Ne result. With increas-

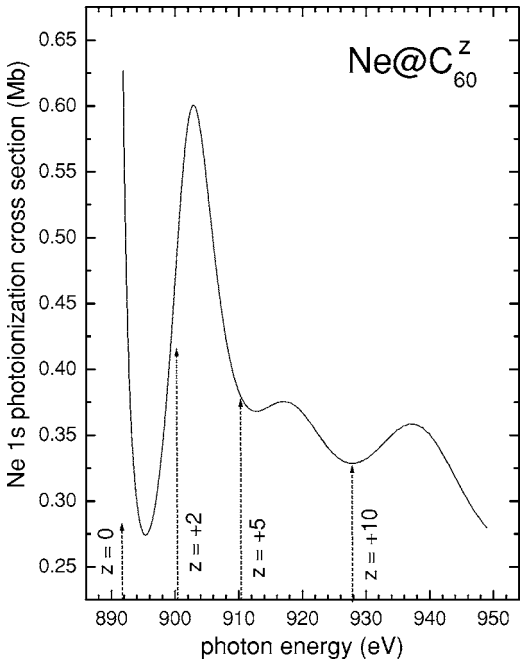

FIG. 6. Calculated HF results for the $\sigma_{1s}(\omega)$ of Ne in neutral Ne@C_{60} (represented by the curve on the whole span of the graph), as well as of Ne in Ne@C_{60}^{+2} (a part of the graph starting at the threshold energy of ≈900 eV and extending towards higher energies), Ne@C_{60}^{+5} (a part of the graph starting at the threshold energy of ≈910 eV and extending towards higher energies), and Ne@C_{60}^{+10} (the part of the graph with a threshold energy of ≈928 eV).

ing negative charge z on C_{60}, the threshold value of $\gamma_{1s}(\omega)$ is shifted to lower photon energies where the additional resonance structure—the Coulomb confinement resonance—is seen at about 887 eV.

From Eq. (9) for $\gamma_{1s}(\omega)$, it is not obvious whether the ordinary confinement resonances or the Coulomb confinement resonances in $\gamma_{1s}(\omega)$ are due to related resonances in the dipole photoionization amplitude D, in the quadrupole photoionization amplitude Q, in phase shifts, or due to a combination of resonance structures. The understanding of the primary avenue through which confinement resonances occur in $\gamma_{1s}(\omega)$ is revealed from an examination of Fig. 5, which makes it clear that both the ordinary and Coulomb confinement resonances in $\gamma_{1s}(\omega)$ arise from the confinement resonances in *quadrupole* photoionization. Indeed, it is seen that $\gamma_{1s}(\omega) \approx \gamma_{1s}(\omega)/\cos\Delta$ [i.e., $\gamma_{1s}(\omega)$ is approximately independent of $\cos\Delta$] and resonances themselves are positioned at precisely the same energies as resonances in the quadrupole photoionization amplitude Q.

B. Photoionization of endohedral cations: Ne@C_{60}^z, $z>0$

In contrast to the case of an endohedral anion Ne@C_{60}^z ($z<0$), the potential $V^{eff}(r)$ seen by a photoelectron due to photoionization of the atom encapsulated in an endohedral cation Ne@C_{60}^z ($z>0$) does not exhibit a Coulomb potential barrier. Although this is quite obvious, yet, for illustration purposes $V^{eff}(r)$, in which a Ne $1s$ photoelectron is moving upon photoionization of the endohedral cation, is shown in Fig. 3 for $z=+5$. Because of the absence of the potential barrier, the photoionization cross section of the atom encapsulated in an endohedral cation must be free of Coulomb confinement resonances. Indeed, this is clearly seen from Fig. 6, where calculated results for $\sigma_{1s}(\omega)$ of Ne in Ne@C_{60}^z are shown for $z=0$, $z=+2$, +5, and +10. In addition, it is seen that charging the shell positively (by removal of some electrons from the neutral C_{60} surface) does nothing to the photoionization cross section (as a function of photon energy) except to increase the threshold energy. The implication is that, in direct opposition to the case of endohedral anions, the only effect of positive C_{60}^z, as compared to neutral C_{60}, is to move some of the oscillator strength of the confined atom from the continuum into the discrete excitation region. Interestingly, this is a precise analogy to the case of *free* positive ions, in which the same effects have been observed [25].

IV. CONCLUSION

The Coulomb confinement resonances in the photoionization cross section as well as in the photoelectron angular asymmetry parameters upon photoionization of the atom encapsulated in endohedral anions, and the redistribution of the oscillator strength of the encapsulated atom between the continuum and discrete spectrum, as predicted for Ne herein, should be general and qualitatively similar for any atom confined by charged C_{60}. We believe that the precise understanding of said features could have important implications in future experimental developments of the spectroscopy of these confined atoms. The data presented herein are intended to promote the initiation of such developments as well.

ACKNOWLEDGMENTS

This work was supported by NSF grants PHY-0456480 and PHY-024394, and NASA NAG5-12712.

[1] H. Shinohara, Rep. Prog. Phys. **63**, 843 (2000).
[2] L. Forró and L. Mihály, Rep. Prog. Phys. **64**, 649 (2001).
[3] W. Harneit, Phys. Rev. A **65**, 032322 (2002).
[4] A. S. Baltenkov, J. Phys. B **32**, 2745 (1999).
[5] J. P. Connerade, V. K. Dolmatov, and S. T. Manson, J. Phys. B **33**, 2279 (2000).
[6] P. Decleva, G. De Alti, and M. Stener, J. Phys. B **32**, 4523 (1999).
[7] J. P. Connerade, V. K. Dolmatov, and S. T. Manson, J. Phys. B **33**, 2279 (2000).
[8] M. Stener, G. Fronzoni, D. Toffoli, P. Colavita, S. Furlan, and P. Decleva, J. Phys. B **35**, 1421 (2002).

[9] M. Ya. Amusia, A. S. Baltenkov, V. K. Dolmatov, S. T. Manson, and A. Z. Msezane, Phys. Rev. A **70**, 023201 (2004).
[10] J. P. Connerade and A. V. Solov'yov, J. Phys. B **38**, 807 (2005).
[11] V. K. Dolmatov, A. S. Baltenkov, J. P. Connerade, and S. T. Manson, Radiat. Phys. Chem. **70**, 417 (2004).
[12] L. Udvari, in *Proceedings of the XIV International Wintershool/Euroconference*, Kirchberg, Tirol (Austria), 2000, edited by H. Kuzmany *et al.* (American Institute of Physics, New York, 2000), AIP Conf. Proc. No. 544, p. 187.
[13] P. Jakes, B. Goedde, M. Wailblinger, N. Weiden, K.-P. Dinse, and A. Weidinger, in *Proceedings of the XIV International Wintershool/Euroconference*, Kirchberg, Tirol (Austria), 2000, edited by H. Kuzmany *et al.* (AIP, New York, 2000), AIP Conf. Proc. No. 544, p. 174.
[14] A. Jánossy, S. Pekker, F. Fülöp, S. Simon, and Z. Oszlányi, in *Proceedings of the XIV International Wintershool/ Euroconference*, Kirchberg, Tirol (Austria), 2000, edited by H. Kuzmany *et al.* (AIP, New York, 2000), AIP Conf. Proc. No. 544, p. 199.
[15] M. Saunders, H. A. Jimenez-Vasques, R. J. Cross, and R. J. Poreda, Science **259**, 1428 (1993).
[16] G. Wendin and B. Wästberg, Phys. Rev. B **48**, 14764 (1993).
[17] J. P. Connerade and R. Semauone, J. Phys. B **33**, 869 (2000).
[18] A. Lyras and H. Bachau, J. Phys. B **38**, 1119 (2005).
[19] T. Almeida Murphy, T. Pawlik, A. Weidinger, M. Hhne, R. Alcala, and J. M. Spaeth, Phys. Rev. Lett. **77**, 1075 (1996).
[20] Y. B. Xu, M. Q. Tan, and U. Becker, Phys. Rev. Lett. **76**, 3538 (1996).
[21] L. S. Wang, J. M. Alford, Y. Chai, M. Diener, and R. E. Smalley, Z. Phys. D: At., Mol. Clusters **26**, S297 (1993).
[22] M. Ya. Amusia and L. V. Chernysheva, *Computation of Atomic Processes: A Handbook for the ATOM Programs* (IOP Publishing, Bristol, 1997).
[23] Oliver Hemmers, Renaud Guillemin, and Dennis W. Lindle, Radiat. Phys. Chem. **70**, 123 (2004).
[24] J. W. Cooper, Phys. Rev. A **47**, 1841 (1993). Note that in Table XII the coefficient $A_{l+1,l-2}$ has the incorrect sign.
[25] S. T. Manson, in *The Physics of Electronic and Atomic Collisions*, edited by A. Dalgarno, R. S. Freund, P. M. Koch, M. S. Lubell, and T. B. Lucatorto (American Institute of Physics, New York, 1990), p. 189.